KSCE Journal of Civil Engineering
DOI 10.1007/s12205-021-0343-z

pISSN 1226-7988, eISSN 1976-3808
www.springer.com/12205

Geotechnical Engineering

Effect of Slime on Engineering Characteristics of Large-Diameter Cast-in-Place Pile

Ong Heo[a], Yeowon Yoon[b], and Jinung Do[c]

[a] Songdo Centrod, Dahyun E&G, Incheon 22007, Korea
[b] *Member,* Dept of Civil Engineering, Inha University, Incheon 22212, Korea
[c] *Member,* Dept of Ocean Civil Engineering, Gyeongsang National University, Tongyeong 53064, Korea

ARTICLE HISTORY

Received 2 March 2021
Revised 30 April 2021
Accepted 25 July 2021
Published Online 14 September 2021

KEYWORDS

Slime
Large-diameter pile
Cast-in-place pile
Uniaxial compressive test
Bi-directional load test
Numerical analysis

ABSTRACT

Slime forms at the bottom of boreholes under the effect of groundwater. The larger the borehole, the more the slime. The demand for large-diameter cast-in-place (CIP) piles has increased as the number of large structures has increased. Excessive slime management can delay construction. However, the effect of slime on the engineering characteristics of large-diameter CIP piles is not understood. In this study, the strength of slime–concrete mixtures was investigated by varying the volume ratio of slime. Field-scale testing was performed to evaluate the behavior of the large-diameter CIP pile using bidirectional load testing. A numerical analysis was performed to assess the compressibility of the slime under the self-weight of the pile. The results revealed that the general levels of slime at the bottom of the borehole had an insignificant influence on the engineering characteristics of the large-diameter CIP pile because the slime is susceptible to being mixed with poured concrete and compressed by the self-weight of the pile.

1. Introduction

The construction of megastructures, such as high-rise buildings, long-span bridges, and large tunnels, has recently increased owing to urban densification and the development of advanced structural materials (Poulos, 2016). Accordingly, the demand for larger foundation systems that can tolerate higher overburden stresses has also increased (Bang et al., 2016). A cast-in-place (CIP) pile is a deep foundation system that can implement a pile with a large diameter (e.g., approximately 2,000 mm) and a deep embedment length (e.g., more than 50 m); thus, it has been widely used for the foundations of large structures (Gao et al., 2017). To implement the CIP pile, a borehole is first made using an auger up to the target depth. If necessary, a casing or drilled fluid is used (Bowles, 1996). Meshed reinforcing bars are inserted into the boreholes. Concrete is poured by using a tremie pipe and hopper to prevent concrete segregation. This CIP pile is classified as a small-, medium-, or large-diameter pile depending on the pile diameter. In addition, the Benoto, earth drill, and reverse circulation drill methods are classified according to their drilling types (Prakash and Sharma, 1990).

When a construction site is under the groundwater level, slime is easily generated at the bottom of the borehole for the CIP pile (Schmertmann et al., 1998). Slime is debris consisting of soil particles, rocks, and water that is induced during the boring process. The type of slime depends on the ground — sandy slime, clayey slime, etc. The existence of slime causes the degradation of concrete quality. The interfacial bonding between the pile surface and the borehole decreases. Finally, the capacity of the pile is impaired (Lam et al., 2014; Lee et al., 2017).

Slime exhibits different behaviors for bored and CIP piles. For the bored pile system, a precast concrete pile is mounted onto the slime. The slime beneath the precast concrete pile may be compressed by the pile and exist at the bottom of the borehole. However, for the CIP pile, slime is mixed with concrete because of the falling energy during the pouring of concrete. Sometimes, a lifting cap (or plunger) is installed in a hopper or tremie pipe before pouring the concrete. The collected concrete stopped by the lifting cap has a higher kinetic energy, so that a stronger impact is applied to slime at the bottom of the borehole resulting in better removal of slime.

Slime can be identified using several approaches, such as a

CORRESPONDENCE Jinung Do jinung@gnu.ac.kr Dept. of Ocean Civil Engineering, Gyeongsang National University, Tongyeong 53064, Korea

visual approach, using penetration resistance, and nondestructive approaches. Using the penetration resistance of slime, a weighted pendulum method is widely employed to identify the presence of slime. A weighted pendulum is lowered into a borehole until the tension of the line connected to the weighted pendulum changes. The weighted pendulum method is likely to depend on the user and operator because the detection of the tension change is manually captured in practice. Ding et al. (2015) and Moghaddam et al. (2018) used a cone-penetrating system to improve the level of slime detection. Chun et al. (2014) and Hong et al. (2020) used an electrical resistivity probe in a borehole with slime and showed that electrical resistivity makes it possible to distinguish the thickness of slime. A visual approach utilizes a special camera called a "shaft inspection device" (SID). The SID is lowered into a borehole, and the presence of slime is identified based on visual observation (Ho, 1982). The SID also has uncertainty in defining slime because the identification is based on changes in the image or turbidity. One example of a nondestructive method is the use of ultrasonic data (called an "ultrasonic drilling monitor system") immediately before boring and immediately before pouring concrete (Chen et al., 2008). However, if slime is rapidly generated during boring and deposition, the accuracy of slime quantification using ultrasonic waves decreases.

Slime can be resolved by direct removal (e.g., hammer grab, mechanical pumping, etc.), blowing removal (air lifting or air blowing), etc. Slime can be indirectly removed by replacing slime with concrete with a falling impact when a hopper and plunger are used. In this case, the slime is mixed with concrete or overflows to the top of the borehole. The slime with rock debris is easy to remove, but clayey and colloidal slime is not. The slime floating in groundwater settles over time. The American Association of State Highway and Transportation Officials recommends maintaining slime at less than 76.2 mm (AASHTO, 2017). However, owing to the uncertainty of slime quantification for removal, the thickness of slime is generally maintained at less than 10% of the pile diameter in practice (based on personal communications with the construction industry). Excessive slime management may slow construction. Research are needed to understand the effect of slime on the engineering properties of deep foundations.

Jun et al. (2009) reported that most slime consists of soil and water, and they evaluated the settling characteristics of an artificial slime (sand:silt:clay = 1:1:1). The sedimentation of the slime was initiated 15 min after mixing, and 95.5% of the final settlement was observed 2 h after mixing. Chun et al. (2014) used electrical resistivity to measure slime. Slime was removed using mechanical pumping, but a new slime was created and eventually remained at the bottom of the borehole. There has been some research regarding the quantification of slime, as mentioned previously; however, few studies have been reported in which the effect of slime on the engineering characteristics of piles, especially large-diameter CIP piles, was evaluated.

In this study, the effect of slime on the engineering characteristics of a large-diameter CIP pile was analyzed. The strength of *in situ* slime–concrete mixtures with a diameter of 100 mm and height of 200 mm was evaluated with respect to uniaxial compression testing. Field testing for large-diameter CIP piles with a diameter of 2,000 mm and length of 63 – 66 m was conducted using bidirectional load testing in the presence of slime, and the behaviors were evaluated. Numerical analyses were performed to examine the compressibility of slime with varying slime thickness (10% – 25% of the pile diameter) under pile weight.

2. Materials and Methods

2.1 Laboratory Testing

2.1.1 Concrete

When concrete is poured into a borehole, slime at the bottom of the borehole is prone to mixing with the concrete. Therefore, the change in the strength of the slime–concrete mixtures was evaluated by varying the volume ratio of slime. Ready-mixed concrete (KS F 4009) was used. The ready-mixed concrete was a Type 1 Portland cement with 25-mm coarse aggregates and a 500-mm slump. Fly ash was used as an additive (20%). The nominal strength of the ready-mixed concrete was 35 MPa.

2.1.2 Slime

In situ slime was collected from the sites for field testing and used for laboratory testing. Two representative slimes were collected: sandy and clayey slimes from two different sites (Fig. 1). Basic geotechnical index tests were conducted, and the properties are summarized in Table 1. Because of the difficulty of consistent sample collection under groundwater, the slime was naturally drained for 24 h at room temperature before measurement and use. The sandy slime had a natural water content (w_n) of 11%, while that of the clayey slime was 29.1%. The specific gravity of the two slimes was 2.6 and 2.7 for the sandy and clayey slimes, respectively (ASTM D854-14, 2014). The sandy slime is nonplastic, while the clayey slime has a liquid limit (w_L) of 42.4% and a plastic limit (w_P) of 21.2% (i.e., plasticity index PI = 21.2%)

Fig. 1. Slimes Collected from Field: (a) Sandy Slime, (b) Clayey Slime

Table 1. Geotechnical Index of Collected Slimes

Type	w_n [%]	G_s	w_L [%]	w_P [%]	USCS
Sandy slime	11.0	2.6	NP	NP	SM
Clayey slime	29.1	2.7	42.4	21.2	CL

(ASTM D4318-17e1, 2017). The slimes were classified as silty sand (SM) and clay with low plasticity (CL) based on a unified soil classification system (USCS) (ASTM D2487-17e1, 2017). Herein, the slimes classified as SM and CL are called "sandy slime" and "clayey slime," respectively.

2.1.3 Uniaxial Compression Testing on Slime–Concrete Mixtures

In practice, slime is usually submerged, so a submerged condition might be suitable for laboratory testing. In this case, slime and concrete are prone to segregation during sample preparation and settlement, making proper evaluation of the mixtures difficult. However, the segregation issue might occur with slow and small concrete pouring. The field testing conducted in this study used a tremie pipe and hopper to induce sufficient kinetic energy during falling to avoid the concrete segregation issue. Therefore, following same mechanism of the field testing, pre-mixed slime-concrete mixtures were used in the laboratory testing. A specimen mold measuring 100 mm in diameter and 200 mm in height was used. Slime was mixed with concrete using a mixer at volume ratios (slime volume over concrete volume, denoted as *V*/*V*) of 0%, 5%, 10%, 15%, and 20%, which are the thicknesses of 0%, 10%, 20%, 30%, and 40%, respectively, compared with the mold diameter. Sandy slime and clayey slime of 110.5 and 77 g, respectively, were required for the volume ratio of 5%. The specimen mold was removed after three days, and the specimen was cured under submerged conditions. After 28-day curing, the specimens were naturally dried, and the top and bottom of the specimen were polished. Uniaxial compression testing was conducted, and the results were analyzed. All specimens were triplicated.

2.2 Field Testing

2.2.1 Test Site

The test site was located in Songdo, Incheon, South Korea. The site consisted of marine sediments and landfills based on a geological map provided by the Korea Institute of Geoscience and Mineral Resources (KIGAM). The bedrock was granite and partially gneiss. Site investigations were implemented at three test sites, denoted as Tests A, B, and C, and the soil profile is shown in Fig. 2. The stratification of the sites was generally landfills (silty sand with gravel) at E.L. of approximately 5 to 15 m, dredged fills (silty sand, silty clay, and sandy silty) at E.L. of approximately -4 to 5 m, marine sediments (clayey and sandy layers) at E.L. of approximately -30 to -4 m, highly weathered rock at E.L. of approximately -30 to -45 m, and moderately weathered rock below E.L. of approximately -45 m. The groundwater table existed at E.L. of approximately 6.25 to 8.1 m.

2.2.2 Test Piles and Bidirectional Load Testing

Three test piles were implemented at sites A, B, and C. The diameter of the pile was 2,000 mm, and the lengths were 66, 66, and 63 m for Tests A, B, and C, respectively. The ready-mixed

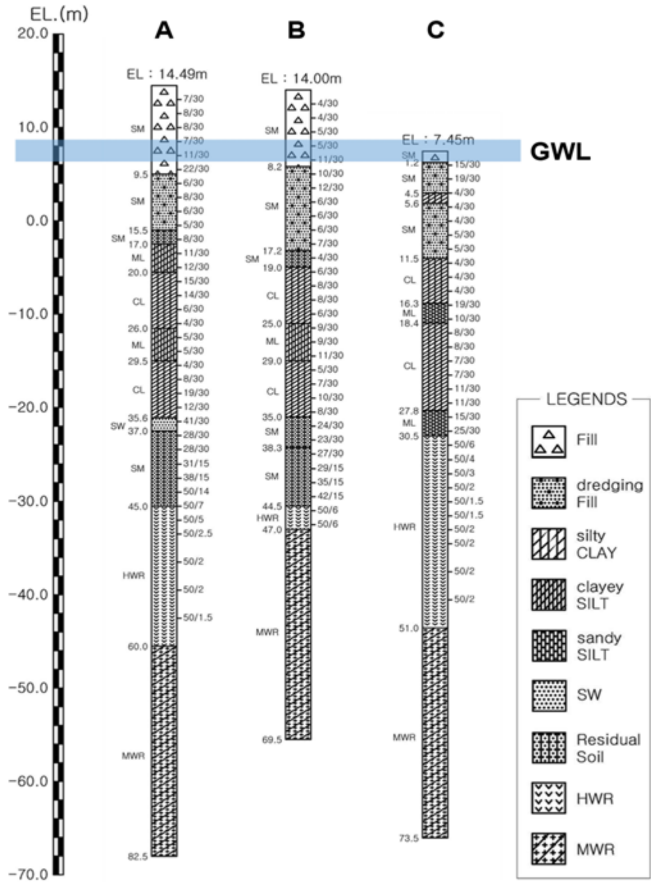

Fig. 2. Stratification of Test Sites

concrete used in the laboratory testing was employed. The slime at the bottom of the borehole was measured using a weighted pendulum. Measuring the thickness of the slime included a certain level of uncertainty because of the groundwater and great depth; however, approximately 300, 250, and 250 mm of slime were estimated for Tests A, B, and C, respectively, which correspond to 15%, 12.5%, and 12.5% of the pile diameter. The test site had the same clayey slime as in Table 1.

Bidirectional load testing was performed to evaluate the behavior of the large-diameter CIP pile. When the meshed reinforcing bar was prepared, a bidirectional load cell was attached to the meshed reinforcing bar 7 m above the bottom of the borehole. Strain gauges were attached to the bar. The sensor cables were protected through a sounding pipe attached to the meshed bar. The equipped bar was inserted into the borehole, and the ready-mixed concrete was poured. After 28-day curing, bidirectional load testing was performed (ASTM D8169M-18, 2018). Loading was applied using a hydraulic pump, and the induced displacement was recorded. Four loading cycles were applied as the rapid loading tests. The maximum load was 52.5 MN. A single cycle consisted of loading and unloading. The first cycle was 0, 6.6, 13.1, 6.6, and 0 MN. The second applied 0, 6.6, 13.1, 19.7, 26.3, 13.1, and 0 MN. The third cycle induced 0, 6.6, 13.1, 19.7, 26.3, 32.8, 39.4, 26.3, 13.1, and 0 MN. The fourth cycle consisted of 0, 6.6, 13.1, 19.7, 26.3, 32.8, 39.4, 45.9, 52.5,

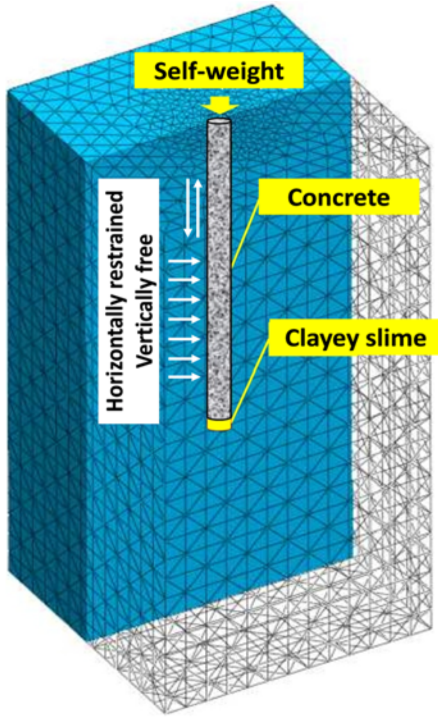

Fig. 3. Modeling of CIP Pile and Slime

39.4, 26.3, 13.1, and 0 MN. The displacement was measured 10 min after reaching the target load, and the maximum load of each cycle was maintained for 20 min. An equivalent load–displacement curve was derived with respect to bidirectional load testing results.

2.3 Numerical Analysis

Numerical analyses were performed to evaluate the behavior of the slime under the weight of the CIP pile (Fig. 3). Commercial software, MIDAS/GTS NX, was used. The total dimensions of the model were 25 × 25 × 100 m (width × length × height) to avoid boundary effect (Bowles, 1996). The borehole was located at the center of the model box, with a 2-m diameter and 66-m height. At the bottom of the borehole, slime was modeled with different thicknesses from 200 to 500 mm in increments of 50 mm. The field testing used a casing to maintain the borehole; therefore, the borehole in the modeling had boundary conditions that were horizontally fixed and vertically free. No vertical load was induced by the superstructure until curing was completed. Thus, only the self-weight of the concrete pile was applied to the slime at the bottom of the borehole. Assuming the unit weight of the CIP pile was 24 kN/m^3, a uniform load of 1,584 kPa (e.g., 24 kN/m^3 × 66 m) was applied to the slime. The bed soil and slime were assumed, based on the site investigations, to be weathered rock and very soft clay. The input properties were obtained from the literature (Das, 2015). Note that the values from the literature are not the ones measured underwater; therefore, the selection of the properties would show a conservative estimation to evaluate the compressibility of the modeled soils. The Mohr–Coulomb model (i.e., elastic and perfectly plastic model) was employed for the bed soil and slime.

3. Results

3.1 Uniaxial Compressive Strength of Slime–Concrete Mixtures

The results of the uniaxial compressive strength (UCS) of the slime–concrete mixtures are shown in Fig. 4. Pure concrete showed an average UCS of 38.3 MPa (37.6, 37.4, and 39.8 MPa) after 28-day curing. The UCS of 38.3 MPa is 9% higher than the nominal UCS of 35 MPa. The UCS was unchanged for a slime volume ratio of 5% – 38.2 and 38.0 MPa for the sandy slime and clayey slime mixtures, respectively. However, the UCS decreased for both the slime–concrete mixtures as the volume ratio of slime increased by more than 5%. For clayey slime–concrete mixtures, the UCS linearly decreased as the volume ratio of slime increased up to 20% *V*/*V* with a UCS of 29.0 MPa. The sandy slime–concrete mixtures showed a similar tendency to that of the clayey slime–concrete mixtures up to 15%. However, at a slime volume ratio of 20%, a higher decrease in UCS was observed (34.6 to 29 MPa from 15% to 20%) than in clayey slime–concrete mixtures (34.3 to 32.90 MPa from 15% to 20%). This implies that the lower water content of the sandy slime (w_n = 11%) reduced the final water/cement ratio of the specimen and eventually lowered the level of the pozzolanic reaction compared with the clayey slime (w_n = 29.1%). However, slime is usually submerged in practice, so the variability of the UCS might be slightly different from that shown in Fig. 4. Overall, both sandy slime and clayey slime decreased the strength of the slime–concrete mixtures as the volume ratio of slime increased. Within a 10% volume ratio of slime, the UCS of the slime–concrete mixtures was 94% – 95% of the UCS of pure concrete.

3.2 Field Testing

3.2.1 Load Transfer along Piles

Figure 5 shows the transferred loads under an applied load of 52.5 MN during the bidirectional load testing. A distance of 0 m indicates the location of the load cell. Because the load cell was

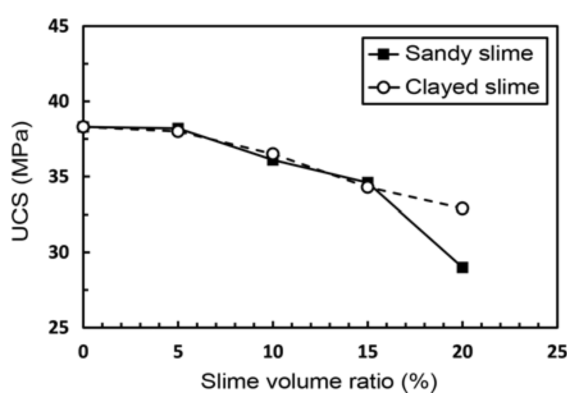

Fig. 4. UCS of Concrete-Slime Mixtures

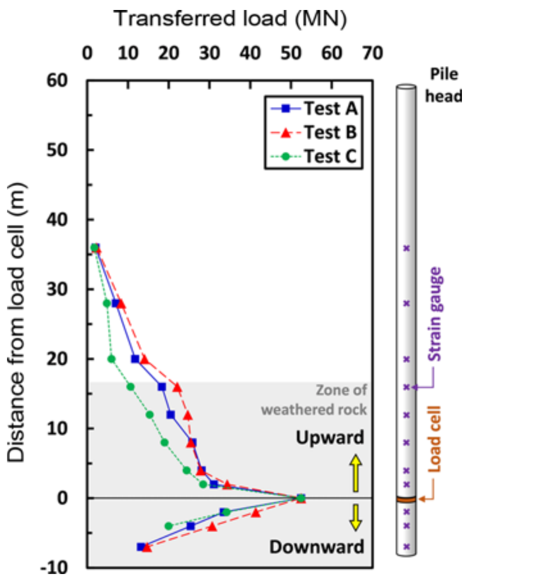

Fig. 5. Transferred Loads along Test Piles at the Applied Load of 52.5 MN

positioned 7 m above the bottom of the borehole, there was a distance of 7 m below the position of the load cell. There was a distance of 59 m for the 66-m pile (Tests A and B) and 56 m for the 63-m pile (Test C) from the load cell. The strain gauges were distributed along 40-m lengths from the end of the pile. The locations of the strain gauges were identical for all the test piles. Fig. 5 indicates that 52.5 MN was applied at the load cell. The closer the distance to the load cell, the higher the transferred load. At an upward distance of 2 m, approximately 30 MN was transferred. The loads were attenuated as the distance from the load cell increased. The transferred load at an upward distance of 36 m was 2 MN. Based on the soil profile, a zone of weathered rock started at a distance from the load cell of approximately 15 m, and the transferred loads showed an inflection curve at a distance of approximately 15 m.

The downwardly transferred loads exhibited a roughly linear attenuation from the load cell. The transferred loads were approximately 20 – 30 MN at a downward distance of -4 m, and approximately 14 MN was observed at the end of the pile. The strain gauge at a -7-m distance for Test C malfunctioned during testing. The trends of the load transfer along the piles were similar to those of Tests A and B. The loads for Test C were lower than those for Tests A and B; however, based on the general trends of all tests, Tests A, B, and C showed similar behaviors. Therefore, it is concluded that the repeatability of the tests is guaranteed.

3.2.2 Bidirectional Load Testing Results

The results of the bidirectional load tests for Tests A, B, and C are plotted in Fig. 6. Because the reference of the displacement is 0, a positive or upward displacement indicates the displacement induced by the loads transferred to the pile skin. A negative or downward displacement indicates the displacement caused by the loads transferred primarily to the pile tip and partially to the

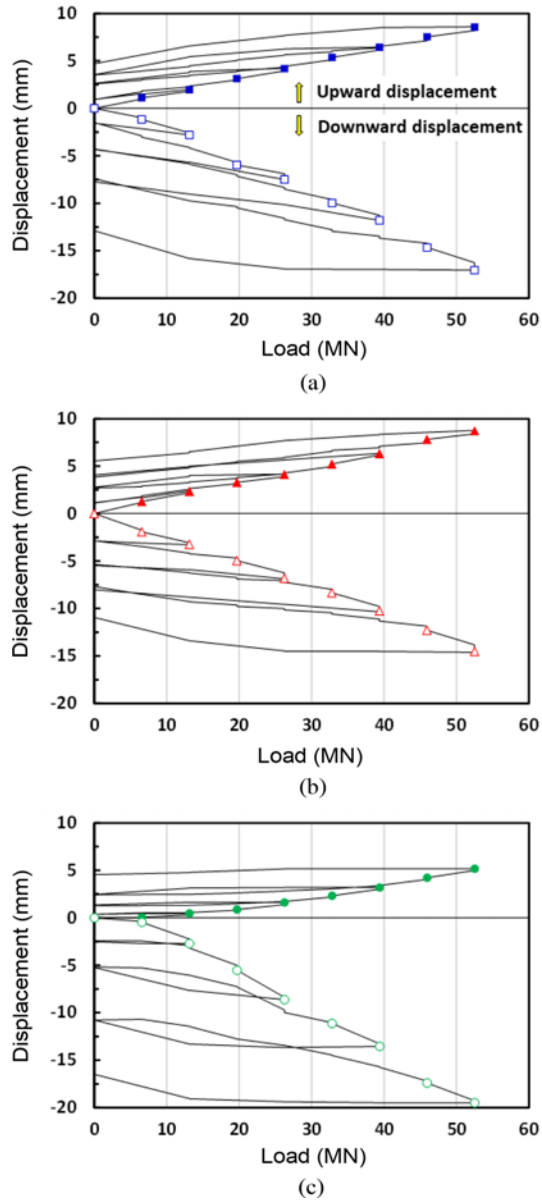

Fig. 6. Results of Bi-directional Load Tests: (a) Test A, (b) Test B, (c) Test C (The upper displacement represents a displacement caused by the load at the pile skin, while the lower displacement is a displacement induced by the load at the pile tip.)

pile skin of 7 m. The displacements increased during the loading and unloading of four loading cycles, and plastic deformations were accumulated. For Test A (Fig. 6(a)), the upward displacement showed a maximum displacement of 8.56 mm at 52.5 MN of the fourth loading cycle, and a plastic deformation of 4.57 mm was observed after the completion of the test. The downward displacement was higher than the upward displacement. A displacement of 17.05 mm (i.e., -17.05 mm) was induced at an applied load of 52.5 MN, and 12.89 mm plastic deformation remained after completion. The observations indicate that the displacement was induced by the loads to the pile tip rather than the pile skin because of the presence of slime at the bottom of the borehole. Tests B (Fig. 6(b)) and C (Fig. 6(c)) were similar to those of Test A (Fig. 6(a)). The displacements of Test B at 52.5 MN were 8.73 and -14.53 mm (Fig. 6(b)), while Test C had 5.17- and -19.49-mm displacements.

The slimes measured before implementing the CIP pile were 300, 250, and 250 mm for Tests A, B, and C, respectively. Considering the effect of groundwater and the uncertainty of the quantification by the weighted pendulum, it can be concluded that the levels of the existing slimes were similar for each borehole. Thus, the range of 5.17 – 8.73-mm upward displacements and the range of 17.05 – 19.49-mm downward displacements can be regarded as analogous. Under testing conditions in which the slimes were as much as 12.5% – 15% of the pile diameter, a total displacement of 75% was induced from the zone of the pile tip because of the presence of the slime at the bottom of the borehole. The general behavior of the pile can be analyzed by means of the following equivalent load–displacement relationship.

3.2.3 Equivalent Load–Displacement Curve from Bidirectional Load Testing Results

Based on the results in Fig. 6, the equivalent load–displacement curves are plotted in Fig. 7. The curves were drawn following the approach presented by Schmertmann et al. (1998). The pile was assumed to be rigid. For a certain level of displacement, the corresponding loads at the upward and downward sides were selected and summed. The summed load represents the equivalent load at the pile head, inducing the designated displacement. Once several equivalent loads were calculated with the selected displacements, the equivalent load–displacement curve was obtained. In this test, there was a limitation in drawing the curve because the downward displacement was three times higher than the upward displacement under the same applied load. In this case, a lower displacement is extrapolated to further displacement (Schmertmann et al., 1998). The upward displacements were extrapolated assuming that no ultimate strength occurred. However, the extrapolation was made up to 15 mm to avoid an excessive prediction.

As shown in Fig. 7, Tests A and B were almost linear and identical within the applied load of 160 MN. The CIP piles of Tests A and B seemed to exhibit elastic behavior within the given loading conditions. Considering the measured slimes of approximately 300 and 250 mm for Tests A and B, respectively, the behaviors of the two CIP piles showed an insignificant difference. The slimes of 250 and 300 mm were 12.5% and 15% of the pile diameter, respectively. Assuming that the slime is mixed with concrete, the 12.5% – 15% slime could be compared with the laboratory testing results for a volume ratio of slime of 6.25% – 7.5% (Fig. 4). The UCS for 5% *V*/*V* slime was similar to that of 0% *V*/*V* slime and thereafter decreased. In the large-diameter CIP pile, the presence of slimes as much as 12.5% – 15% the thickness of the pile diameter would have had an insignificant influence on the pile behavior.

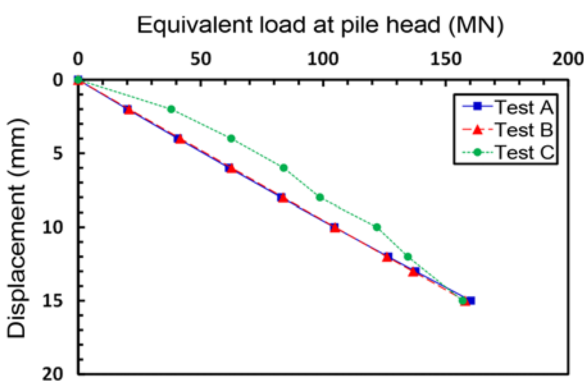

Fig. 7. Equivalent Load-Displacement Curve from Bi-directional Load Testing Results

Test C showed a nonlinear behavior compared with Tests A and B. Test C showed a higher resistance up to the equivalent load of 150 MN and merged with Tests A and B at 160 MN with approximately 15-mm displacements. The upward and downward displacements at 52.5 MN for Test C were 5.17 and -19.49 mm, respectively (Fig. 6(c)), which are lower and higher, respectively, than those of Tests A (8.56 and -17.05 mm) and B (8.73 and -14.53 mm). This observation can be attributed to the spatial variability of the test sites; however, the general load–displacement relationships could be deemed to be insignificantly different within the given range.

The absence of a control pile (i.e., a CIP pile with no slime) is a limitation in this field testing for comparison. However, a perfectly clean bottom without slime in the borehole was unavailable in practice because of the presence of groundwater and floating particles in the borehole. Nonetheless, despite the presence of slimes as much as 12.5% – 15% the thickness of the pile diameter, the large-diameter CIP piles behaved elastically. A low level of slime is susceptible to mixing with poured concrete. The strength of the slime–concrete mixtures is not significantly different from that of pure concrete in the case of approximately 10% *V*/*V* slime. Therefore, it can be concluded that the levels of slimes existing at the bottom of the borehole (12.5% – 15% the thickness of the pile diameter) do not have a critical impact on the behavior of the large-diameter CIP pile.

3.3 Numerical Analysis

The results of the numerical analyses are summarized in Table 2, and an example of the numerical analyses is shown in Fig. 8. The thickness of the slime varied from 200 to 500 mm, corresponding to 10% – 25% of the pile diameter. The results indicate the compressibility of the slime at the bottom of the borehole under the self-weight of the pile. When the self-weight of the pile was 1,584 kPa, the entire zone of the slime was removed from the original for slime thicknesses of 200 – 450 mm. For instance, for

Table 2. Input Parameters for Modeling

Parameters	γ_t [kN/m^3]	c [kPa]	ϕ [°]	E [MPa]	v
Bed soil	20	30	33	750	0.3
Slime	14	15	0	2	0.3

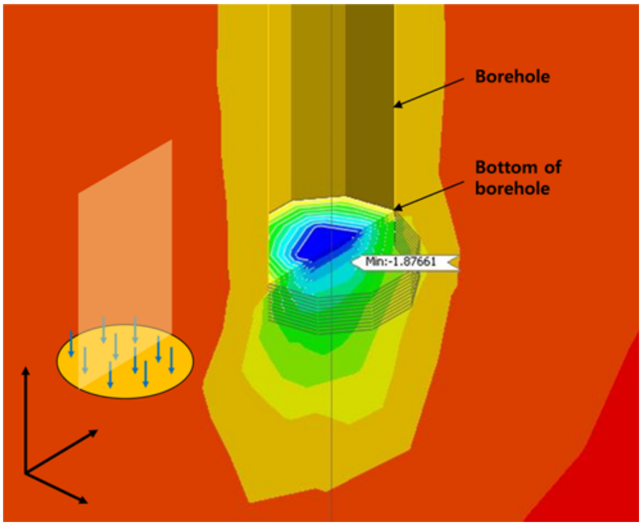

Fig. 8. Half Space of the Modeling with the Deformation under Self-weight of the Pile (The maximum displacement occurs at the center of the borehole.)

Table 3. Numerical Analysis Results

Slime thickness [mm]	Total deformation [mm]
200	249
250	297
300	346
350	390
400	428
450	460
500	487

a slime thickness of 200 mm (10% of the pile diameter), the total deformation was 249 mm. Most deformation was attributed to slime, in addition to a partial deformation of the bed soil. The compressed slime spread spherically to the bed soil (Fig. 8). The deformation took place beyond the original zone of the slime until the slime thickness was 450 mm. When the slime thickness was 500 mm (25% of the pile diameter), the total deformation was 487 mm. The deformation of the slime was approximately 485 mm, while the bed soil was compressed by approximately 2 mm (-1.88 mm, as shown in Fig. 8). The results suggest that most of the slimes used in this analysis were compressed and spread to the surrounding soil under the self-weight of the pile.

The mechanism of the CIP pile on the slime is different from that of the bored pile. The slime of the bored pile is compressed. The slime in the CIP pile was mixed or overflowed. Laboratory testing showed that the slime–concrete mixture with 10% *V*/*V* slime was insensitive to the strength. The numerical analysis revealed that most slime of as much as 25% the pile diameter was compressed owing to the pile weight. Therefore, it is concluded that the problem of slime for the large-diameter pile can be resolved by either mixing with concrete or being compressed by the self-weight of the pile when slime is within a manageable range.

4. Conclusions

This study investigated the effect of slime on the engineering properties of a large-diameter CIP pile. The strength of the slime–concrete mixtures was evaluated by assuming that the slime was mixed with poured concrete. Field testing was conducted to examine the behavior of large-diameter CIP piles in the presence of slime at the bottom of the borehole. The compressibility of the slime under the self-weight of the pile was evaluated with a numerical analysis. The results are summarized as follows.

1. The strength of the slime–concrete mixtures showed an insignificant difference from that of pure concrete when the volume ratio of slime was 5%. Slime–concrete mixtures had a strength greater than the nominal strength of concrete up to 10% *V*/*V* slime. In general, the strength of the slime–concrete mixtures decreased as the volume ratio of slime increased.
2. Large-diameter CIP piles elastically behaved despite the presence of clayey slime of 12.5% – 15% the pile diameter. The estimated slime might be mixed with poured concrete and can be negligible. This observation supports the guideline that slime should be less than 76.2 mm or 10% of the pile diameter.
3. Numerical analyses showed that most slimes of large-diameter piles are compressed under the self-weight of the pile for slime up to 25% of the pile diameter.
4. Overall, the general level of slime existing at the bottom of boreholes (~15% the pile diameter) causes an insignificant influence on the engineering characteristics of either a CIP or a bored pile. Therefore, excessive maintenance to eliminate the slime at the bottom of boreholes would be unnecessitated.

Acknowledgments

Funding from Gyeongsang National University Office of Academy and Industry Collaboration and Marine Industry Research Center is appreciated. We would like to thank Editage (www.editage.co.kr) for English language editing.

ORCID

Jinung Do https://orcid.org/0000-0003-4568-2781

References

AASHTO (2017) LRFD Bridge construction specifications, 4th edition. American Association of State Highway and Transportation Officials, Washington DC, USA

ASTM D854-14 (2014) Standard test methods for specific gravity of soil solids by water pycnometer. ASTM D854-14, ASTM International, West Conshohocken, PA, USA

ASTM D2487-17e1 (2017) Standard practice for classification of soils for engineering purposes (unified soil classification system). ASTM D2487-17e1, ASTM International, West Conshohocken, PA, USA

ASTM D4318-17e1 (2017) Standard test methods for liquid limit, plastic limit, and plasticity index of soils. ASTM D4318-17e1, ASTM International, West Conshohocken, PA, USA

ASTM D8169M-18 (2018) Standard test methods for deep foundations under bi-directional static axial compressive load. ASTM D8169M-18, ASTM International, West Conshohocken, PA, USA

Bang JW, Park CK, Yang SY, Kim YY (2016) Flexural behavior of large-diameter composite PHC pile using in-filled concrete and reinforcement. *Journal of the Korea Institute for Structural Maintenance and Inspection* 20(5):109-115, DOI: 10.11112/jksmi.2016.20.5.109

Bowles LE (1996) Foundation analysis and design. McGraw-Hill Education, New York, NY, USA

Chen XY, Shen J, Zhu J, Wang W, Qian DG (2008) Design of ultrasonic drilling monitor system. *Instrument Technique and Sensor* 5

Chun OH, Yoon HK, Park MC, Lee JS (2014) Slime thickness evaluation of bored piles by electrical resistivity probe. *Journal of Applied Geophysics* 108:167-175, DOI: 10.1016/j.jappgeo.2014.07.004

Das BM (2015) Principles of foundation engineering. Cengage Learning, Boston, MA, USA

Ding JZ, McIntosh KA, Simon RM (2015) New device for measuring drilled shaft bottom sediment thickness. *Journal of the Deep Foundations Institute* 9(1):42-47, DOI: 10.1179/1937525515Y.0000000004

Gao L, Yang K, Chen X, Yu X (2017) Study on the deformation measurement of the cast-in-place large-diameter pile using fiber bragg grating sensors. *Sensors* 17(3):505, DOI: 10.3390/s17030505

Ho R (1982) Development of a shaft inspection device. *Transportation Research Board* 102

Hong WT, Woo G, Park MC, Lee JS (2020) Slime-meter for assessment of slime thickness based on electrical properties in borehole. *Automation in Construction* 119:103328, DOI: 10.1016/j.autcon.2020.103328

Jun S, Park B, Lee H, Yoo N, Moon M (2009) Engineering characteristics of slime generated by application of deep mixing method. *Journal of the Korean Geo-Environmental Society* 10:99-103

Lam C, Jefferis SA, Martin CM (2014) Effects of polymer and bentonite support fluids on concrete-sand interface shear strength. *Geotechnique* 64(1):28-39, DOI: 10.1680/geot.13.P.012

Lee JH, Cho JW, Do J, Park B (2017) Evaluation of field applicability of cast-in-place piles using surfactant grout. *Key Engineering Materials* 744:207-213, DOI: 10.4028/www.scientific.net/KEM.744.207

Moghaddam RB, Hannigan PJ, Anderson K (2018) Quantitative assessment of drilled shafts base-cleanliness using the shaft quantitative inspection device (SQUID). Proceedings of IFCEE 2018, March 5-10, Orlando, FL, USA

Poulos HG (2016) Tall building foundations: Design methods and applications. *Innovative Infrastructure Solutions* 1(1), DOI: 10.1007/s41062-016-0010-2

Prakash S, Sharma HD (1990) Pile foundations in engineering practice. John Wiley & Sons, Hoboken, NJ, USA

Schmertmann JH, Hayes JA, Molnit T, Osterberg LO (1998) O-cell testings case histories demonstrate the importance of bored pile (drilled shaft) construction technique. Proceedings of 4th international conferences on case histories in geotechnical engineering, March 8-15, St. Louis, MO, USA